Ninth Canadian Conference on Earthquake Engineering
Ottawa, Ontario, Canada
26-29 June 2007

MODIFIED OPERATOR SPLITTING METHOD FOR COLLABORATIVE STRUCTURAL ANALYSIS SYSTEM

M. Tada[1] and P. Pan[2]

ABSTRACT

The collaborative structural analysis (CSA) system is capable of performing highly sophisticated structural analyses utilizing the beneficial features of existing individual structural analysis programs. This requires a time consuming static condensation procedure if adopting an implicit integration scheme. The operator splitting (OS) method, which does not request tangential stiffness, can be used to improve the system efficiency. Furthermore, the conventional OS method is not able to provide enough numerical stability particularly for the analyses considering geometrically nonlinearity, and improvement is needed. To this end, a modified OS method, which treats unbalanced forces in the current step as pseudo external forces in the immediate following step, is proposed.

Introduction

A collaborative structure analysis system is proposed by Tada et al (2004), which is capable of performing highly sophisticated structural analysis by utilizing the beneficial features of existing individual structural analysis programs developed by individual research. In the system, the simulated structure is divided into multiple substructures, and each substructure is analyzed by an individual program. Specifically, the host program formulates and solves the equilibrium equations or equations of motion for the entire structure, and sends boundary displacements to the corresponding station programs. The station programs run detailed analyses, and return the stiffnesses and forces associated with the degrees of freedom (DOFs) at the boundaries through a condensation procedure. The procedure is conducted step by step, and the data are exchanged through the Internet. The system has the following characteristics:

1) Multiple existing programs can be used for sophisticated structural analysis collaboratively. Flexible combinations are available for specific analysis projects according to the project characteristics and requirements.

2) Only data for analysis projects need to be exchanged over the Internet, whereas sharing source codes or running libraries of existing programs are unnecessary so that the copyrights of the programs are firmly protected.

[1]Assoc. Professor, Div. of Global Architecture, Graduate School of Engineering, Osaka University, Suita City, Japan
[2]JSPS Fellow, Graduate School of Engineering, Kyoto University, Kyoto City, Japan

3) Basically only the input and output of the existing programs need modification for a specific analysis project, so that the efforts are minimized.

4) The sharing files and folders technique, which can be implemented by Fortran 77 for most of the operating system, is used for the data exchange over the Internet. The method is so common that it is applicable for most Internet environment supporting TCP/IP protocol.

5) Tight collaborations are needed among the researchers taking care of station programs for modeling, data input, and result investigation since the researchers taking care of some station programs do not necessarily understand the entire system. In other words, the programs are not used as black boxes for such collaborations.

6) How to divide the analyzed structure into substructures, and how to choose station programs depend on the expected behavior of the simulated structure, thus requiring engineering experience. For this reason, the proposed system is not suitable for investigating the behavior of a completely unknown structural system.

To investigate the applicability of the collaborative analysis system, Tada distributes multiple programs (all developed by the author) into 10 locations around Japan for pushover and time history analyses of a three storey braced steel moment frame (Tada 2004). To demonstrate the effectiveness of the system, another three projects are conducted, and details are given in Tada and Ohgami (2004), Tada and Tamai (2004), and Pan (2005). Specifically, in Tada and Ohgami (2004), a local buckling analysis program (NASP) developed by Ohgami and a composite beam analysis program (COMPO) developed by Tada are chosen as station programs, and NETLYS also developed by Tada is adopted as host program. Collaborative pushover analyses are conducted also for a three story braced steel moment frame. In Tada and Tamai (2004), an exposed column base analysis program developed by Tamai is added to the collaborative analysis system consisting NASP, COMPO, and NETLYS, and pushover and time history analyses are conducted for the same steel structure adopted in Tada and Ohgami (2004). In Pan (2005), an online hybrid test of an eight storey base-isolated structure is simulated by using the collaborative system, in which the base-isolation layer is physically tested, and the superstructure is numerically simulated by NETLYS.

In the above collaborative analyses or online hybrid tests, the stiffness of a substructure is firstly condensed to the DOFs associated with the boundaries, and sent from the station to the host. In the host program, the stiffness matrices obtained from substructures are assembled to formulate the stiffness matrix of the entire structure, which is used for the incremental analysis. However, if the DOFs of the substructure solved by a station program are very large, the condensation procedure requires large computational efforts. In addition, the protection of commercial source codes for structural analyses is too strict for common users to be modified for the condensation procedure, which makes it unsuitable for the collaborative system. Furthermore, in the online hybrid tests, estimation of the tangential stiffness matrix for tested substructure is difficult mainly because of the control and measurement error existing in physical test.

Online hybrid tests treat part of the substructures experimentally, while the others numerically. A few effective time integration algorithms (Takanashi 1980, Nakashima 1990, and Kanda 1995), which only use restoring forces but do not need stiffness matrix, have been proposed for online hybrid tests, and the operator-splitting (OS) method is one of them. Development of a new OS algorithm suitable for the collaborative system is the main target of this study. By using this algorithm, general-purposed structural analysis programs and experimental facilities can be easily incorporated as station programs since condensation procedure and data exchange over the Internet for stiffness matrices are not needed any longer.

In this study, the disadvantages of the conventional OS algorithms are firstly investigated based on sophisticated analyses considering geometric nonlinearity. Then an improved algorithm is proposed. In addition, the quasi-static pushover analysis and the time history analysis for a three-story braced frame are carried out by the collaborative system employing the new OS algorithm, in which a general-purposed structural analysis program, i.e. ABAQUS, is incorporated as a station program. Here, the sophisticated analysis of the square-tube column base connected by brace is analyzed by ABAQUS; whereas the analysis of the global frame including the buckling behavior of the braces is implemented by the host program, i.e. NETLYS. The feasibility and effectiveness of the collaborative system, which simulate the entire frame behavior by combining the detailed substructure analyses results, is demonstrated.

Incremental Formulation of Conventional OS Method

The OS method is a hybrid time integration method proposed by Hughes (Hughes 1979), in which the stiffness of a structure is split into a history-independent linear part, and a history-dependent nonlinear part. An implicit time integration method is employed for the linear part, and an explicit method is used for the nonlinear part. In Nakashima (1990), the OS method is implemented for a substructural analysis, in which parts of the structure are tested physically, and the rest are analyzed numerically. Specifically, the explicit predictor-corrector method is taken for the integration associated with the nonlinear stiffness, whereas the unconditionally stable Newmark-β method is employed for the integration associated with the linear stiffness. In Nakashima (1990), the OS method was formulated in a total form. It will be reformulated into an incremental form in this study.

According to the formulation of OS method proposed in Nakashima (1990) (referred to as the conventional OS method hereafter), the equation of motions for Step n+1 is:

$$[\mathbf{M}]\{\mathbf{a}_{n+1}\}+[\mathbf{C}]\{\mathbf{v}_{n+1}\}+[{}_{\mathbf{I}}\mathbf{K}]\{\mathbf{d}_{n+1}\}+\left(\{\mathbf{f}_{n+1}\}-[{}_{\mathbf{I}}\mathbf{K}]\left\{\tilde{\mathbf{d}}_{n+1}\right\}\right)=\{\mathbf{P}_{n+1}\} \tag{1}$$

Where, $\{\mathbf{a}_{n+1}\}$: acceleration vector for Step **n+1**; $\{\mathbf{v}_{n+1}\}$: velocity vector for Step **n+1**; $\{\mathbf{d}_{n+1}\}$: corrector displacement vector for Step **n+1**; $\{\tilde{\mathbf{d}}_{n+1}\}$: predictor displacement vector for Step **n+1**; $\{\mathbf{f}_{n+1}\}$: resorting force vector corresponding to predictor displacement for Step **n+1**; $\{\mathbf{P}_{n+1}\}$: external force vector for Step **n+1**; [**M**]: mass matrix; [**C**]: damping matrix; $[{}_{\mathbf{I}}\mathbf{K}]$: initial stiffness matrix.

The predictor displacement vector $\{\tilde{\mathbf{d}}_{n+1}\}$ is given in Eq. (2), which is obtained explicitly from displacement, velocity, and acceleration vector of Step **n**.

$$\left\{\tilde{\mathbf{d}}_{n+1}\right\}=\{\mathbf{d}_n\}+\left\{\Delta\tilde{\mathbf{d}}_n\right\},\quad \left\{\Delta\tilde{\mathbf{d}}_n\right\}=\Delta\mathbf{t}\{\mathbf{v}_n\}+\frac{\Delta\mathbf{t}^2}{4}\{\mathbf{a}_n\} \tag{2), (3}$$

where, $\Delta\mathbf{t}$ is time interval.

Furthermore, according to the Newmark-β method, corrector displacement and velocity satisfy the following assumptions:

$$\{\mathbf{d}_{n+1}\}=\{\mathbf{d}_n\}+\Delta\mathbf{t}\{\mathbf{v}_n\}+\frac{\Delta\mathbf{t}^2}{4}\{\mathbf{a}_n\}+\frac{\Delta\mathbf{t}^2}{4}\{\mathbf{a}_{n+1}\},\quad \{\mathbf{v}_{n+1}\}=\{\mathbf{v}_n\}+\frac{\Delta\mathbf{t}}{2}\left(\{\mathbf{a}_n\}+\{\mathbf{a}_{n+1}\}\right) \tag{4), (5}$$

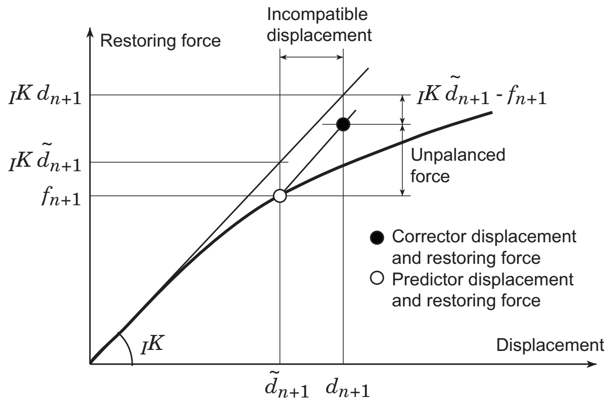

Figure 1. Conventional OS method in total form.

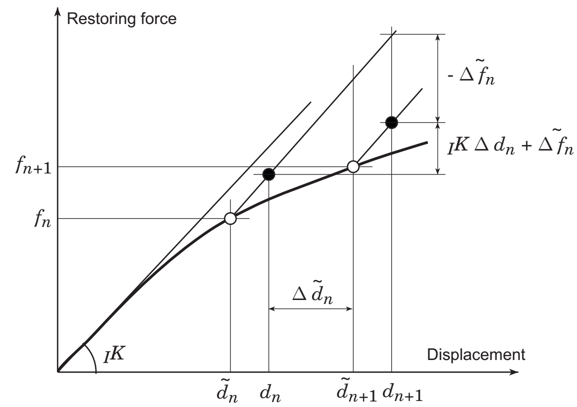

Figure 2. Conventional OS method in incremental form.

In Eq. (1), the first and second terms on the left hand side are the inertia and damping forces, respectively, and the third and the fourth terms represent the restoring force. The restoring force is illustrated in Fig. 1. In the figure, $\{\tilde{\mathbf{d}}_{\mathbf{n+1}}\}$ is the predictor displacement, which is calculated explicitly from information of Step **n**, and $\{\mathbf{f}_{\mathbf{n+1}}\}$ is the corresponding restoring forces. The difference of restoring forces between the corrector displacements $\{\mathbf{d}_{\mathbf{n+1}}\}$ and the predictor displacements $\{\tilde{\mathbf{d}}_{\mathbf{n+1}}\}$ is approximately represented by $[_I\mathbf{K}]$ ($\{\mathbf{d}_{\mathbf{n+1}}\}$ - $\{\tilde{\mathbf{d}}_{\mathbf{n+1}}\}$) using initial stiffness matrix $[_I\mathbf{K}]$.

On the other hand, the equations of motion for Step **n** are expressed as follows:

$$[\mathbf{M}]\{\mathbf{a_n}\}+[\mathbf{C}]\{\mathbf{v_n}\}+[_I\mathbf{K}]\{\mathbf{d_n}\}+\left(\{\mathbf{f_n}\}-[_I\mathbf{K}]\left\{\tilde{\mathbf{d}}_\mathbf{n}\right\}\right)=\{\mathbf{P_n}\} \tag{6}$$

Subtracting both sides of Eq. (6) from Eq. (1), the equations of motion in an incremental form are obtained as

$$[\mathbf{M}]\{\Delta\mathbf{a_n}\}+[\mathbf{C}]\{\Delta\mathbf{v_n}\}+[_I\mathbf{K}]\{\Delta\mathbf{d_n}\}+\left\{\Delta\tilde{\mathbf{f}}_\mathbf{n}\right\}=\{\Delta\mathbf{P_n}\} \tag{7}$$

where,

$$\{\Delta\mathbf{d_n}\}=\{\mathbf{d_{n+1}}\}-\{\mathbf{d_n}\},\quad \{\Delta\mathbf{v_n}\}=\{\mathbf{v_{n+1}}\}-\{\mathbf{v_n}\},\quad \{\Delta\mathbf{a_n}\}=\{\mathbf{a_{n+1}}\}-\{\mathbf{a_n}\} \qquad \text{(8a, b, c)}$$

$$\{\Delta\mathbf{P_n}\}=\{\mathbf{P_{n+1}}\}-\{\mathbf{P_n}\},\quad \left\{\Delta\tilde{\mathbf{f}}_\mathbf{n}\right\}=\{\mathbf{f_{n+1}}\}-\{\mathbf{f_n}\}-[_I\mathbf{K}]\left(\left\{\tilde{\mathbf{d}}_\mathbf{n+1}\right\}-\left\{\tilde{\mathbf{d}}_\mathbf{n}\right\}\right) \qquad \text{(9), (10)}$$

The incremental restoring force $[_I\mathbf{K}]$ $\{\Delta\mathbf{d_n}\}$ + $\{\Delta\tilde{\mathbf{f}}_\mathbf{n}\}$ used in Eq. (7) is further illustrated in Fig. 2. Solving Eqs. (8a,c) for $\{\mathbf{d_{n+1}}\}$ and $\{\mathbf{a_{n+1}}\}$, and substituting them to Eq. 4, $\{\Delta\mathbf{d_n}\}$ can be easily obtained as

$$\{\Delta\mathbf{d_n}\}=\Delta\mathbf{t}\{\mathbf{v_n}\}+\frac{\Delta\mathbf{t}^2}{2}\{\mathbf{a_n}\}+\frac{\Delta\mathbf{t}^2}{4}\{\Delta\mathbf{a_n}\} \tag{11}$$

Similarly, solving $\{\mathbf{v_{n+1}}\}$ and $\{\mathbf{a_{n+1}}\}$ from Eqs. (8b,c), and substituting them to Eq. 5, $\{\Delta\mathbf{v_n}\}$ can be easily obtained as

$$\{\Delta\mathbf{v_n}\}=\Delta\mathbf{t}\{\mathbf{a_n}\}+\frac{\Delta\mathbf{t}}{2}\{\Delta\mathbf{a_n}\} \tag{12}$$

Using Eqs. (11) and (12), $\{\Delta\mathbf{a_n}\}$ and $\{\Delta\mathbf{v_n}\}$ can be written as

$$\{\Delta a_n\}=-2\{a_n\}-\frac{4}{\Delta t}\{v_n\}+\frac{4}{\Delta t^2}\{\Delta d_n\},\qquad \{\Delta v_n\}=-2\{v_n\}-\frac{2}{\Delta t}\{\Delta d_n\} \tag{13), (14}$$

Substituting $\{\Delta \mathbf{a_n}\}$ and $\{\Delta \mathbf{v_n}\}$ in Eqs. (13) and (14) to Eq. (7), the relation between $\{\Delta \mathbf{d_n}\}$ and $\{\Delta \mathbf{P_n}\}$ can be easily solved as

$$\left(\frac{4}{\Delta t^2}[M]+\frac{2}{\Delta t}[C]+[_IK]\right)\{\Delta d_n\}=[M]\left(2\{a_n\}+\frac{4}{\Delta t}\{v_n\}\right)+2[C]\{v_n\}-\left\{\Delta\tilde{f}_n\right\}+\{\Delta P_n\} \tag{15}$$

Modified OS Method by Compensating Unbalanced Force

In the conventional OS method, the restoring force of $\{\mathbf{f_{n+1}}\}$ (shown by a white circle in Fig. 1) corresponds to the predictor displacement $\{\tilde{\mathbf{d}}_{\mathbf{n+1}}\}$ of the Step **n+1**; and the restoring force of $\{\mathbf{f_{n+1}}\}$ + $[_I\mathbf{K}]$ ($\{\mathbf{d_{n+1}}\}$ - $\{\tilde{\mathbf{d}}_{\mathbf{n+1}}\}$) (shown by a black circle in Fig. 1) corresponds to the corrector displacement $\{\mathbf{d_{n+1}}\}$. Although neither the corrector state nor the predictor state satisfies the compatibility and the equilibrium conditions, the incompatible displacement and the unbalanced force are so small that they are negligible for engineering purposes. Error in the incompatible displacement will not accumulate in the conventional OS method because it is corrected by the incremental displacement compensation [refer to Eq. (2)], and consequently the unbalanced force is corrected indirectly. In this study, a new OS method (referred to as the modified OS method hereafter), which avoids error accumulation by force compensation, is proposed. In this method, the unbalanced force is reversed and applied as the additional external force in next step analysis. In this way, incremental displacement is obtained by compensating the unbalanced force so that it is indirectly corrected. Specifically, the modified OS method is as follows:

In this method, different to that given in Eq. (2), since direct compensations are not for displacement, the predictor displacement for Step **n+1** is defined as

$$\left\{\tilde{d}_{n+1}\right\}=\left\{\tilde{d}_n\right\}+\left\{\Delta\tilde{d}_n\right\} \tag{16}$$

Furthermore, in reference to Fig. 3, the equations of motion in an incremental form can be written as Eq. (17) since the unbalanced force $\{_{\mathbf{unb}}\mathbf{P_n}\}$ generated at Step **n** is applied as reverse pseudo-external force in Step **n+1**:

$$[M]\{\Delta a_n\}+[C]\{\Delta v_n\}+\{\Delta_{out}P_n\}=\{\Delta P_n\} \tag{17}$$

$$\{\Delta_{out}P_n\}=\{_{out}P_{n+1}\}-\{_{out}P_n\}=[_IK]\{\Delta d_n\}+\left\{\Delta\tilde{f}_n\right\}-\{_{unb}P_n\} \tag{18}$$

where, $\{_{\mathbf{unb}}\mathbf{P_n}\}$ equals to the restoring force corresponding to the corrector displacement $\{_{\mathbf{out}}\mathbf{P_n}\}$ minus that corresponding to the predictor displacement $\{\mathbf{f_n}\}$, and is defined as:

$$\{_{unb}P_n\}=\{_{out}P_n\}-\{f_n\} \tag{19}$$

Replacing **n** in Eqs. (18) and (19) by **n-1**, $\{_{\mathbf{unb}}\mathbf{P_n}\}$ can be easily derived as

$$\{_{unb}P_n\}=\{f_{n-1}\}+[_IK]\{\Delta d_{n-1}\}+\left\{\Delta\tilde{f}_{n-1}\right\}-\{f_n\} \tag{20}$$

Utilizing $\{\Delta \mathbf{a_n}\}$ in Eq. (13) , $\{\Delta \mathbf{v_n}\}$ in Eq. (14), the relation between $\{\Delta \mathbf{d_n}\}$ and $\{\Delta \mathbf{P_n}\}$ can be easily solved as

$$\left(\frac{4}{\Delta t^2}[M]+\frac{2}{\Delta t}[C]+[{}_IK]\right)\{\Delta d_n\}=[M]\left(2\{a_n\}+\frac{4}{\Delta t}\{v_n\}\right)+2[C]\{v_n\}-\{\Delta\tilde{f}_n\}+\{{}_{unb}P_n\}+\{\Delta P_n\} \quad (21)$$

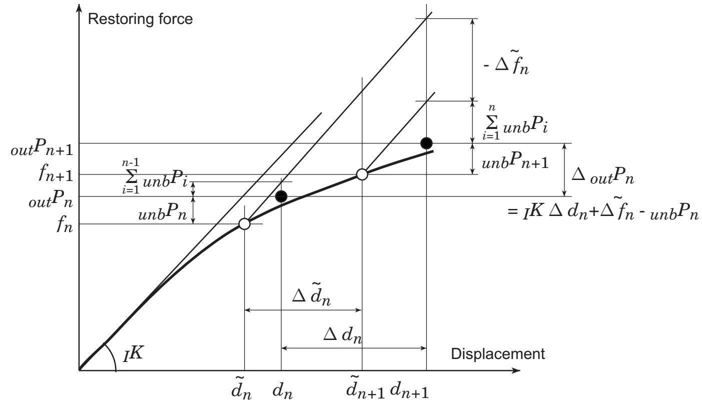

Figure 3. Modified OS method

Dynamic Force-Displacement Relationship of Cantilever Column Using OS Algorithm

The force-displacement relationship of a cantilever column as shown in Fig. 4 is calculated using the method proposed in the previous sections. A forced displacement is imposed on the top of the cantilever column with a constant speed. The column is divided into two parts at the position of 700 mm away from the fixed end. The upper part is analyzed using the Newmark-β method, while the lower part by the OS method. The cross-section of the column is RHS (350mm high and 12mm thick). A mass of 1000 kN in weight is assigned on the top of the column. There's no mass on the boundary. The natural period is 0.427 sec. At the boundary, the inertia force is zero, but the damping force is nonzero and it is taken into account in the equations of motion. The initial stiffness proportional to damping is adopted, and a critical damping ratio of 2% is assigned to the first vibration mode. It takes 200 steps to push the top of the column to 100 mm in the horizontal direction with a constant speed of 40 mm/s. The steel material model is defined with a Young's modulus of 205 kN/mm^2, yielding strength of 0.325 kN/mm^2, and hardening ratio of 0.0001. The plasticity behavior of the column base is determined by the combined effects of the axial force and moment.

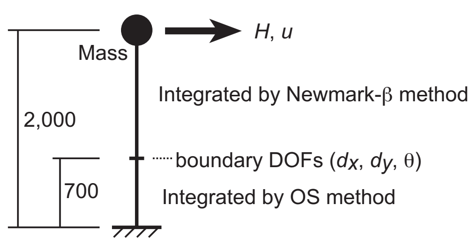

Figure 4. Simple example structure of a single column.

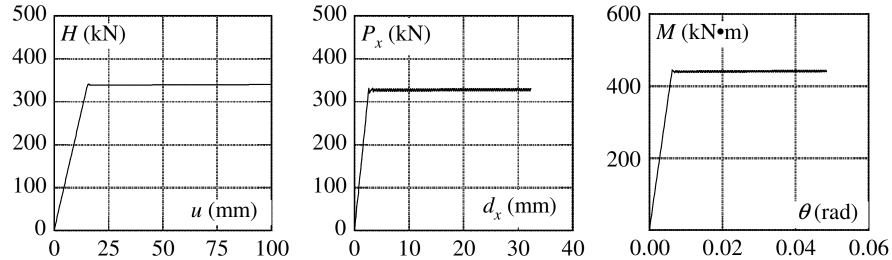

(a) Conventional OS method

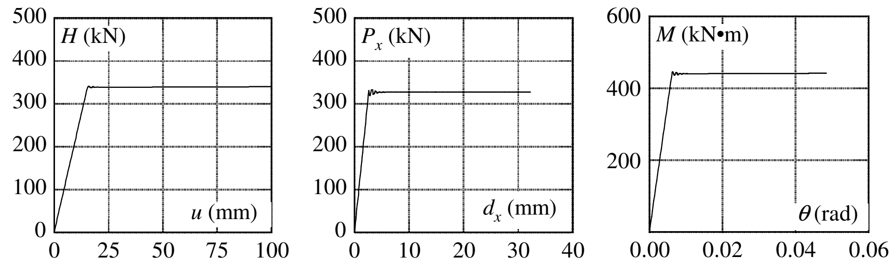

(b) Modified OS method

Figure 5. Excluding geometrical nonlinearity.

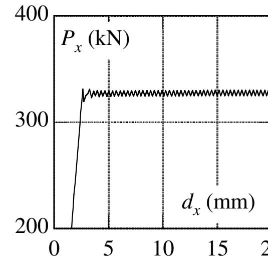

Figure 6. Enlarged Px-dx.

The analysis results without considering geometric nonlinearity are shown in Fig. 5. The results from two analysis algorithms are compared. The results of the conventional OS algorithm (using incompatible displacement compensation) proposed in (Nakashima 1990) are shown in Fig. 5 (a), while the results of the modified algorithm in this study (using unbalanced force compensation) are shown in Fig. 5 (b). The following relationships are compared for the two algorithms: (1) horizontal force on the top of the column (**H**) – horizontal displacement (**u**); (2) horizontal force at the boundary (**P_x**) – horizontal displacement (**d_x**); and (3) moment at the boundary (**M**) – rotation angle (**θ**). For the **H-u** relationship, the two algorithms are almost the same. For the **P_x-d_x** relationship and the **M-θ** relationship, the two algorithms by and large are the same. However, if observed closely, there is significant difference between the two algorithms. For example, the **P_x-d_x** relationship obtained from the method using the incompatible displacement compensation is enlarged in Fig. 6. It can be clearly observed that zigzag occurs after plastification. This phenomenon also happens in the **M-θ** relationship. In Fig. 5, this zigzag is shown like a thick line. On the other hand, in the results using the unbalanced force compensation, several vibrations occur around the yielding point for both the **P_x-d_x** and the **M-θ** relationships, but they all damp very soon and converge to a smooth horizontal lines. If using the conventional OS algorithm in which incompatible displacement is compensated, the zigzag phenomenon has little influence on the global behavior because this numerical error only occurs locally. Comparing with this, the zigzag never happens if using the modified algorithm to compensate the unbalanced force.

The results considering geometric nonlinearity are shown in Fig. 7. The force-displacement relationship derived by Jennings (1968), which considers the axial deformation due to bending deformation, is employed for the members sustaining axial force and moment simultaneously. The geometric stiffness matrix is calculated as the multiplication of the initial stress of each step, by the partial-differenced transformation matrix from local coordinator system to global system with respect to the displacement on the top of the column. In the analyses, the equilibrium condition is satisfied for the post-deformation status considering the geometric stiffness matrix. Similar to Fig. 5, the results using the incompatible displacement compensation are shown in Fig. 7 (a), while the results using the unbalanced force compensation are shown in Fig. 7 (b). The vertical force ($\mathbf{P_y}$)-displacement ($\mathbf{d_y}$) relationship on the boundary is also shown in the right of Fig. 7. Note that vertical force-displacement relationship dose not exist if geometric nonlinearity is not considered. In the case using incompatible displacement compensation, the amplitude of the zigzag after plastification increases significantly and diverges in the end. Especially for the $\mathbf{P_y}$-$\mathbf{d_y}$ relationship, the amplitude increases to the yielding strength in the tension direction. Contrast to this, in the case using the modified OS algorithm, which adopts unbalanced force compensation, a stable behavior can be traced when even considering geometric nonlinearity.

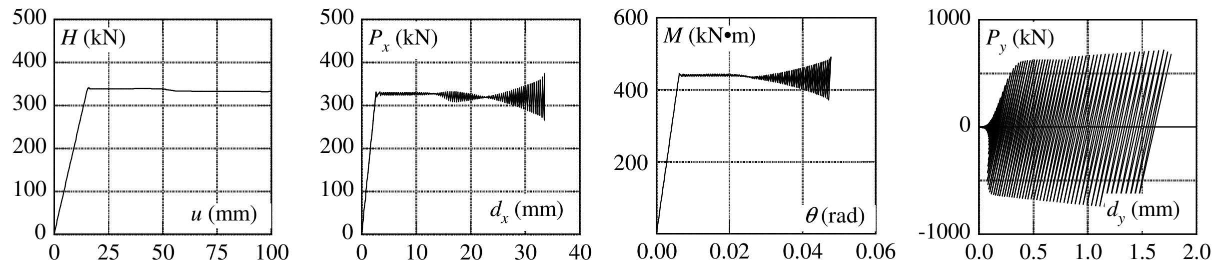

(a) Conventional OS method

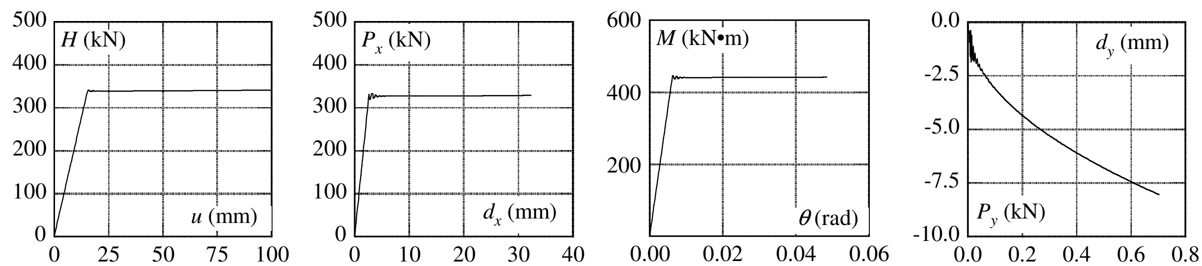

(b) Modified OS method

Figure 7. Including geometrical nonlinearity.

In reference (Nakashima 1990), θ was defined for the relationship between initial stiffness ($\mathbf{K^I}$) and tangential stiffness ($\mathbf{K}$) as: $\mathbf{K^I = \theta\ K}$. If $\theta \geq 1$, OS algorithm was proven unconditionally stable. The analyses in this study show that the stiffness of the vertical DOF on the boundary appear to be negative when considering geometric nonlinearity. In this case, θ is negative too, and the unconditional stable condition is not satisfied. On the other hand, according to the previous analyses, the behavior of the vertical degree of freedom at the boundary has no effect on the global behavior if geometric nonlinearity is not considered. Therefore, it is believed that the geometric nonlinearity is the reason that leads the algorithm using incompatible displacement compensation to diverge. The mathematical demonstration, however, will be a research topic in the future.

Collaboration of General-Purposed Structural Analysis Program and Frame Analysis Program

In this collaborative structural analysis application using the modified OS method, the general-purposed structural analysis program, i.e. ABAQUS, is used as the station program, and a frame analysis program, i.e. NETLYS, is employed as the host program. Geometric nonlinearity is taken into account. The square tube column base is analyzed by ABAQUS sophisticatedly. The local buckling introduced by the axial force and the moment, and the stress concentration for the gusset plate connected to the brace are analyzed in detail. The global behavior of the frame is analyzed by considering these effects. The modified OS method is employed for the part to be analyzed by ABAQUS, and the Newmark-β method is used for the part to be analyzed by NETLYS. In addition, it is verified that the analysis result using the conventional OS method cannot be completed due to the divergence.

Analytical frame

As shown in Fig. 8, analyzed structure is a three story steel braced frame. The cross-sections of components are listed as follows: Beam: wide flange (300mm high, 200mm wide, 6mm thick in web, 12mm thick in flange); Column: RHS (350mm high, 12mm thick); Middle column connected to braces: wide flange (300mm high, 300mm wide, 9mm thick in web, 16mm thick in flange); Brace: CHS (200mm high, 4mm thick). The yielding strength of steel is 0.325 kN/mm^2. The beam of each 9-meter span is divided equally to 6 elements. Associated lumped mass and gravity are assigned for each node of the beams. The gravity and the seismic loads are given in Table.1 and Fig. 8. The horizontal load distribution for pushover analysis is similar as the seismic load for the preliminary design ($\mathbf{H_i}$ as shown in Fig. 8): $\mathbf{H_3}$ = 819.5 kN, $\mathbf{H_2}$ = 465.0 kN, $\mathbf{H_1}$ = 324.5 kN. In order to simulate the buckling behavior of the braces, a middle node is added to each brace member, and its nodal coordinates are adjusted so that the corresponding brace has an initial imperfection of 1/1000 of the length. Note that it is difficult to trace the equilibrium path for a brace member with a critical slenderness ratio after static buckling in the axial direction. Therefore, a mass equal to the total mass of the brace member is assigned to the middle node to consider the dynamic equilibrium in the direction orthogonal to the axis of the brace member. The plastification for members, i.e. columns, beams and braces is judged by the yielding surface considering combined effects of axial and bending loads. Panel zone is considered by a pure shear model with yielding shear strength of 0.250 kN/mm^2. Kinematical hardening is considered for members and panel zone with the hardening ratio of 0.0001. The fundamental period of the structure is 0.4145 sec. Initial stiffness proportional damping is considered, and a critical damping ratio of 2% is assigned to the first vibration mode. Here, the inertial force for the node without mass is zero, but the damping force is included.

Table 1. Loading condition (kN).

	floor	P_1	P_2	P_3
vertical load	roof	144.3	212.5	28.0
	3F	153.1	207.0	31.2
	2F	155.0	207.5	31.7
vertical load for seismic force estimation	roof	139.1	202.2	27.3
	3F	138.5	177.7	28.9
	2F	140.4	178.3	29.5

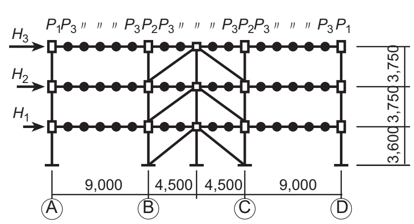

Figure 8. Example structure

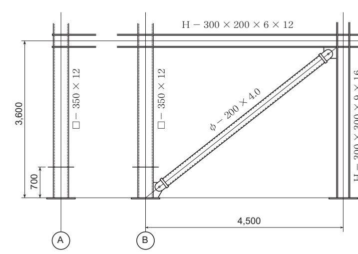

Figure 9. Details of frame (mm)

Substructure to be analyzed by general-purposed structural analysis program

Fig. 9 shows details of the frame. The column bases to be analyzed by ABAQUS are shown in Fig. 10, in which the base of an exterior column is shown in Fig. 10 (a), and the base of interior column connected to brace is shown in Fig. 10 (b). As shown in Fig. 10 (a), the translation in **x**, **y** direction and the rotation ($\mathbf{x_c}$, $\mathbf{y_c}$, $\boldsymbol{\theta_c}$) at the top of the column are the boundary DOFs, which are connected to the super frame analyzed by the host program. In Fig. 10 (b), in addition to the above three components, the boundary DOFs include two translations ($\mathbf{x_b}$, $\mathbf{y_b}$) at the pin connected to the brace.

The column bases are modeled by a three-dimensional thick shell element S4R in ABAQUS. S4R is a 4-node, quadrilateral, stress/displacement shell element with reduced integration and a large-strain formulation. Bilinear behavior with kinematical hardening is considered for steel material nonlinearity, and the hardening ratio is taken to be 0.001. Geometric nonlinearity is considered in the analyses. Convergence study is conducted for the subassemblies to determine the mesh before the collaborative analyses.

Wang and Pan (2005) succeed in the time history analysis of a multiple story frame, in which the frame model was analyzed statically by ABAQUS, the mass-spring model was used for simulating dynamics by a homemade program, and the horizontal displacements and corresponding restoring forces are transferred between the two models. The similar technique is employed in this study. The increment displacement is sent to ABAQUS from the host program (NETLYS). After ABAQUS analysis, the restoring force is fed back to the host.

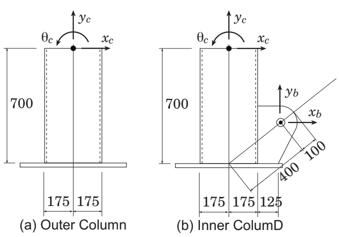

Figure 10. Column base

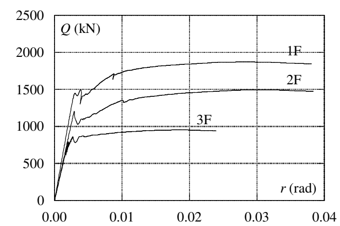

Figure 11. **Q-r** relation

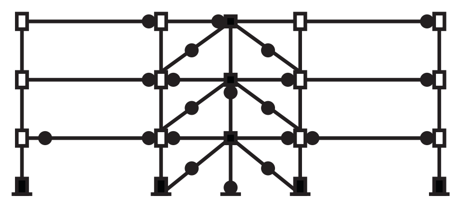

Figure 12. Distribution of plastic hinges

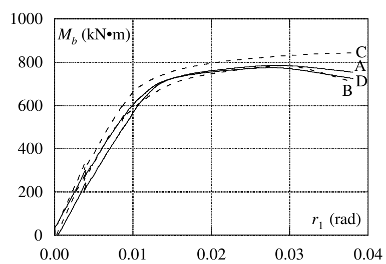

Figure 13. $\mathbf{M_b}$-$\mathbf{r_1}$ relation at column base.

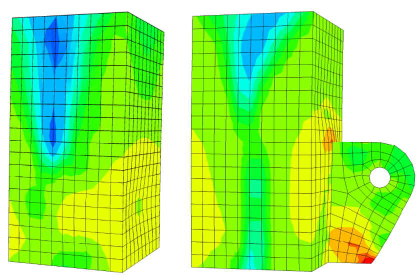

Figure 14. Column base deformation.

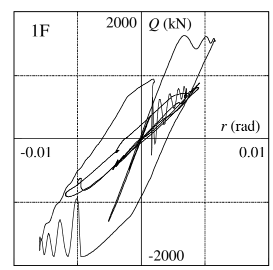

Figure 15. **Q-r** relation at the first story.

Quasi-static pushover analysis and time history analysis

Pushover analysis is helpful to understand the essential force-displacement characteristics of structures. In order to use the OS method, which does not require stiffness, quasi-static pushover analyses using displacement control with slow enough velocity are conducted. Gravity load is first applied in 0.4 sec by 50 incremental steps. Then the top floor of the structure is pushed to 370 mm, under the proportional horizontal forces to seismic design forces, in 8 sec by 1000 incremental steps. In the above loadings, a single incremental step uses 0.008 sec, which is about 1/50 of the fundamental period of the structure.

The story shear (**Q**) and story drift angle (**r**) relation is plotted in Fig. 11. The plastification distribution of the final state is shown in Fig. 12. All the column bases sustain intensive plasticity, most of the beams yields, and all the braces buckles at the middle points. In Fig. 11, the story shear strength increases and reaches the extreme at about 1/300 story drift angle, sharply drops due to the brace buckling, recovers again with the further increase of story drift angle, and finally degrades after reaching the maximum strength. The relationship between the column base moment ($\mathbf{M_b}$) and the first story drift angle ($\mathbf{r_1}$) is given in Fig. 13. Solid lines (A and D) represent the bases of two exterior columns. Dotted lines (B and C) represent the bases of two interior columns. The relation shows notable strength degradation of the column base due to local buckling. Fig. 14 shows the deformation shape and corresponding stress distribution of the column bases. The out-of-plane deformation occurs at the flanges sustaining compression, and the stress concentration at the gusset plate is significant. In this study, these two phenomena do not affect the global behavior of the entire frame significantly, although they are considered in the analysis.

Time history analysis is also carried out using El Centro NS with the maximum ground velocity of 50 cm/s and the duration shorten to 5 sec. A time interval of 0.002 sec is adopted. The fist story shear and story drift angle relation is given in Fig. 15. The figure clearly shows the vibration behavior due to the brace buckling.

Conclusions

In this study, the OS algorithm is incorporated into the collaborative structural analysis system. For this reason, it is possible to coordinate the host and station programs, and only the restoring forces (without the stiffness matrices) of substructures using sophisticated models are sent from the station to the host. It is found easy to combine various station tools including general-purposed structural analysis programs, and test facilities. The major findings obtained from this study are as follows.

(1) The conventional OS algorithm satisfies neither the compatibility condition nor equilibrium condition at the states corresponding to the predictor and the corrector. However, the error is commonly negligible for engineering purposes. The conventional OS algorithms avoid the error accumulation by incompatible displacement compensation in each step.

(2) The conventional OS algorithms correct the incompatible displacement, which involves a zigzag. If geometric nonlinearity is taken into consideration, the zigzag may increase, leading the analysis to diverge.

(3) The modified OS algorithm based on the unbalanced force compensation is formulated. It is verified that a stable solution can be obtained for the analyses even considering geometric nonlinearity.

(4) In the collaborative structural analysis system used in this study, the OS algorithm with unbalanced force compensation is employed, and a general-purposed structural analysis program, ABAQUS, is incorporated. Using the system, the pushover and the time history analyses of a three-story braced frame are conducted successfully.

Acknowledgments

Financial support by the Ministry of Education, Culture, Sports, Science and Technology of Japan under Grant No. 16560498, and those by National Research Institute for Earth Science and Disaster Prevention for the NEES/E-Defense collaborative research, are gratefully acknowledged.

References

Hughes, T.J.R., K.S. Pister, and R.L. Taylor, 1979. Implicit-Explicit Finite Elements in Nonlinear Transient Analysis, *Computer Methods in Applied Mechanics and Engineering*, pp. 159-182.

Jennings, A., 1968. Frame Analysis Including Change of Geometry, *Proc. of ASCE*, No.ST4, pp.627-644.

Kanda, M., H. Adachi, N. Shirai, and M. Nakanishi, 1995. Implicit Integration Scheme Based on Initial Stress Method for Substructure On-Line Test, *Journal of Structural and Construction Engineering*, No.473, pp. 75-81 (in Japanese).

Nakashima, M., T. Kaminosono, M. Ishida, and K. Andp, 1990. Integration Techniques for Substructure Pseudo Dynamic Test, *In 4th US National Conference on Earthquake Engineering*, Palm Springs, CA.

Pan, P., M. Tada, and M. Nakashima, 2005. Online Hybrid Test by Internet Linkage of Distributed Test-Analysis Domains, *Earthquake Engineering and Structural Dynamics*, Vol. 34, pp.1407-1425.

Tada, M. and A., 1998. Suito: Static and Dynamic Post-Buckling Behavior of Truss Structures, Engineering Structures, Vol. 20, Nos 4-6, pp384-389.

Tada, M. and S. Kuwahara, 2004. Fundamental Study on Unified Tool for Structural Analysis Using Network, *Proceedings of 13th World Conference on Earthquake Engineering*, Paper No. 650, CD-ROM

Tada, M. and K. Ohgami, 2004. Internet-Based Numerical Analysis of Steel Building Frame in Collaboration of Frame Analysis and Local Buckling Analysis, *Proc. of the 6th Korea-Taiwan-Japan Joint Seminar on Earthquake Engineering for Building Structures*, pp.201-206.

Tada, M. and H. Tamai, 2006. Collaborative Structural Analysis Linking Programs of Composite Beam and Column Base, *Proceedings of STESSA 2006, Behavior of Steel Structures in Seismic Areas*.

Takanashi, K., K. Odagawa, and H. Tanaka, 1980. Non-linear Earthquake Response Analysis of Structures by a Computer-Actuator On-line System, *Journal of Structural and Construction Engineering*, No.288, pp. 115-123. (in Japanese).

Wang, T., P. Pan, H. Tomofuji, M. Nakashima, and M. Ohsaki, 2005. Online Hybrid Test Combined with General-Purpose Finite Element Program, *Journal of Structural Engineering*, Vol. 51B, pp.261-268.